

SEP 20 2002

TAMU-HAL-2002-001

**INFLUENCE OF SURFACE ROUGHNESS  
AND FREESTREAM TURBULENCE ON THE  
SECOND ORDER TRANSPORT OF  
TURBULENCE IN NON-EQUILIBRIUM  
BOUNDARY LAYERS**

**Dr. Rodney D. W. Bowersox**

**Aerospace Engineering and Mechanics  
The University of Alabama  
Tuscaloosa, AL 35487**

**SEPTEMBER 2002**

**FINAL REPORT FOR PERIOD 01 JANUARY 2001 – 30 JUNE 2002**

**Approved for Public Release; Distribution Unlimited**

**20021031 016**

# REPORT DOCUMENTATION PAGE

AFRL-SR-AR-TR-02-

Public reporting burden for this collection of information is estimated to average 1 hour per response, including the time for reviewing instructions, searching existing data sources, gathering the required data, completing and reviewing this collection of information. Send comments regarding this burden estimate or any other aspect of this collection of information, including suggestions for reducing the burden, to Washington Headquarters Services, Directorate for Information Operations and Reports (0704-014302). Respondents should be aware that notwithstanding any other provision of law, no person shall be subject to any penalty for failing to comply with a collection of information if it does not have a valid OMB control number. PLEASE DO NOT RETURN YOUR FORM TO THE ABOVE ADDRESS.

1. REPORT DATE (DD-MM-YYYY) 20-09-2002		2. REPORT TYPE Final Report		3. DATES COVERED (From - To) 01-01-2001 30-06-2002	
4. TITLE AND SUBTITLE The Influence of Surface Roughness and Freestream Turbulence on the Second Order Transport of Turbulence in Non-Equilibrium Boundary Layers				5a. CONTRACT NUMBER F49620-01-1-0115	
				5b. GRANT NUMBER	
				5c. PROGRAM ELEMENT NUMBER	
				5d. PROJECT NUMBER	
6. AUTHOR(S) Rodney D. W. Bowersox, Ph.D.				5e. TASK NUMBER	
				5f. WORK UNIT NUMBER	
				8. PERFORMING ORGANIZATION REPORT NUMBER  TAMU-HAL-2002-001	
7. PERFORMING ORGANIZATION NAME(S) AND ADDRESS(ES)  The University of Alabama Aerospace Engr. & Mechanics Box 870280 Tuscaloosa, AL 35487				10. SPONSOR/MONITOR'S ACRONYM(S)	
9. SPONSORING / MONITORING AGENCY NAME(S) AND ADDRESS(ES) AFOSR/NA 801 N. Randolph St., Rm. 732 Arlington, VA 22203-1977				11. SPONSOR/MONITOR'S REPORT NUMBER(S)	

12. DISTRIBUTION / AVAILABILITY STATEMENT  
Approved for Public Release; Distribution Unlimited

13. SUPPLEMENTARY NOTES

20021031 016

## 14. ABSTRACT

This document describes the results of AFOSR Grant F49620-01-1-0115, which was a one-year project to bridge the gap between AFOSR Grants F49620-98-1-0038 and F49620-02-1-0365. The objectives of the grant F49620-01-1-0115 were to design and construct Mach 3.0 rough-wall, favorable pressure-gradient test sections and perform wind tunnel tests. Ten favorable pressure gradient models were designed and constructed. However, testing was not accomplished. Instead, to continue progress, numerical simulations were performed. First, algebraic roughness models, which were previously validated by the PI for flat-plate flows, were incorporated into a parabolized Navier-Stokes solver, and simulations of the smooth and rough wall supersonic favorable pressure gradient flows were accomplished. Second, additional simulations were performed with the Wilcox k-w model using the Aerosoft, Inc. CFD code GASP.

## 15. SUBJECT TERMS

Rough-Wall, Boundary Layer, Turbulence, Supersonic

16. SECURITY CLASSIFICATION OF:			17. LIMITATION OF ABSTRACT  SAR	18. NUMBER OF PAGES	19a. NAME OF RESPONSIBLE PERSON Rodney Bowersox
a. REPORT Unclassified	b. ABSTRACT Unclassified	c. THIS PAGE Unclassified			19b. TELEPHONE NUMBER (include area code) (205) 845-1669

# EXECUTIVE SUMMARY

This document describes the results of AFOSR Grant F49620-01-1-0115, which was a one-year project to bridge the gap between AFOSR Grants F49620-98-1-0038 and F49620-02-1-0365. In the earlier grant, the PI performed a detailed investigation of the effects of roughness on a flat plate boundary layer. The results from that study were disseminated to the Air Force through the final report, numerous journal publications, contractor meetings and conference presentations; e.g., see Latin and Bowersox (1999, 2000, 2002), Fan and Bowersox (1999) and Pritchett and Bowersox (2001). The focus of the follow-on project is improved flow field understanding for the combined effects of surface roughness, freestream turbulence and streamline curvature driven pressure gradients.

The specific objectives of this grant (F49620-01-1-0115) were to design and construct Mach 3.0 favorable pressure gradient test sections and to perform wind tunnel tests. Ten favorable pressure gradient models were designed and constructed. The model design and fabrication required more time than was anticipated. Hence, testing was not accomplished. However, the models transitioned to Texas A&M University with the PI for work on the follow-on project. Instead, and to continue progress, the PI performed numerical simulations of the smooth and rough wall supersonic favorable pressure gradient flows with (1) a parabolized Navier-Stokes solver using algebraic roughness models validated for flat plate flows by Fan and Bowersox (2001) and (2) the Wilcox (2001)  $k-\omega$  model, using the CFD code GASP.

The expected technology transitions from this effort are tied to the follow-on project. First, the test matrix was defined with Air Force flow regimes in mind. Hence, the database itself will be useful for model validation and practical engineering design. Second, fundamental information is to be acquired with the goal of providing improved understanding of the flow physics, which will ultimately lead to improved prediction methods. As an example, the data generated in the AFOSR Grant F49620-98-1-0038, as reported in Latin and Bowersox (2000), were used to validate current numerical methods being used to design the hypersonic nozzle for the Air Force AEDC RDHWT/MARIAH II project.

# List of Tables

<u>TABLE 1 FREESTREAM FLOW CONDITIONS</u> .....	19
<u>TABLE 2 FAVORABLE PRESSURE GRADIENT WALL COORDINATES</u> .....	25

# List of Figures

FIGURE 1 FLOW FIELD SCHEMATIC.....	23
FIGURE 2 PHOTOGRAPHS OF THE TEST SECTION AND SURFACE ROUGHNESS TOPOLOGIES .....	24
FIGURE 3 SEMI-CIRCULAR GROOVE PATTERN FOR ALL OF THE ROUGHNESS ELEMENTS [IN. (MM)] .....	24
FIGURE 4 FAVORABLE PRESSURE WALL GEOMETRY.....	24
FIGURE 5 MACH DISTRIBUTIONS WITHIN THE FPG TEST SECTIONS .....	28
FIGURE 6 SHEAR STRESS DISTRIBUTIONS (ALGEBRAIC MODELS) .....	28
FIGURE 7 LAW-OF-THE-WALL RESULTS, K- $\omega$ MODEL WITHOUT COMPRESSIBILITY SCALING) .....	29

# Table of Contents

<u>EXECUTIVE SUMMARY</u> .....	I
<u>LIST OF TABLES</u> .....	II
<u>LIST OF FIGURES</u> .....	III
<u>LIST OF FIGURES</u> .....	III
<u>TABLE OF CONTENTS</u> .....	IV
<u>TABLE OF CONTENTS</u> .....	IV
<b>1. INTRODUCTION</b> .....	1
1.1 DOCUMENTED AIR FORCE RELEVANCE .....	1
1.2 RESEARCH REQUIREMENT .....	2
1.3 RESEARCH OBJECTIVES .....	2
1.4 SUMMARY OF PROGRESS.....	3
1.5 TECHNOLOGY TRANSITIONS .....	4
<b>2. BACKGROUND REVIEW</b> .....	5
2.1 SMOOTH FLAT PLATE TURBULENT BOUNDARY LAYERS WITH LOW TURBULENCE .....	5
2.2 ROUGH FLAT PLATE TURBULENT BOUNDARY LAYERS WITH LOW TURBULENCE .....	6
2.3 EFFECT OF PRESSURE GRADIENT/WALL CURVATURE ON SMOOTH-WALL BOUNDARY LAYERS .....	9
2.4 EFFECT OF TURBULENCE INTENSITY ON LOW-SPEED TURBULENT BOUNDARY LAYERS .....	14
2.5 LIMITATIONS OF CURRENT PREDICTION METHODS.....	16
<b>3. FACILITIES AND APPARATUS</b> .....	19
3.1 WIND TUNNEL FACILITIES .....	19
3.2 COMPUTATIONAL RESOURCES .....	19
<b>4. RESULTS</b> .....	21
4.1 WIND TUNNEL MODELS.....	21
4.2 NUMERICAL RESULTS .....	25
<b>5. BIBLIOGRAPHY</b> .....	30

# 1. Introduction

## 1.1 Documented Air Force Relevance

The US Air Force (1995), in the *New World Vistas* document, identified viscous drag reduction and increased aircraft engine performance as key enabling technologies for the advancement of future war fighting technologies. Internal and external flow fields associated with modern weapons systems are very complicated. The complications include compressibility, pressure gradients, wall curvature, high Reynolds numbers, elevated turbulence levels, surface roughness and combustion. The US Air Force Office of Scientific Research, in the Turbulence and Rotating Flows Section of the AFOSR BAA 2001-1 (December 1999) document, solicited basic research in turbulence applicable to Air Force airbreathing propulsion and advanced flight systems. Of specific relevance to this research, the AFOSR BAA listed as important (1) improved turbulence modeling approaches for highly strained turbulent environments, with emphasis in incorporating the physics of turbulence into the predictive models, and (2) high quality turbulent flow data relevant to the advancement of transport and subgrid models for high Reynolds number flow. This research program is focused on these two documented Air Force Office of Scientific Research requirements.

The improved physical understanding targeted in this multi-grant project has direct relevance for numerous ongoing Air Force Research Laboratory propulsion development programs, e.g., (1) the Integrated High Performance Turbine Engine Technology (IHPTET) program, (2) the Hypersonic Technologies (HyTech) program, (3) Integrated High Payoff Rocket Propulsion Technology program, and (4) the RDHWT/MARIAH II Project.

Access-to-space vehicle development (also listed in the AFOSR BAA) will also benefit from this research. Specifically, the thermal protection systems currently used for exterior aerodynamic and interior propulsion include ceramics, molded RTV, molded cork etc., all of which exhibit surface roughness and streamline curvature.

## **1.2 Research Requirement**

The Background section of this document (Chapter 2) demonstrates that accurate prediction of the influence of surface roughness and freestream turbulence on non-equilibrium compressible turbulent boundary layer flow over curved surfaces is a scientifically challenging problem, and as mentioned in Section 1.1 this problem has numerous important Air Force applications. Numerical limitations prevent DNS or LES simulations for wall-bounded flows, and eddy-viscosity methods have proven to be poor representations of the flow physics. Hence, the remaining modeling options are models founded in the second order transport equations for the terms explicitly appearing in the Reynolds or Favre averaged form of the Navier-Stokes equations. Because of the complicated nature of the equations, empirical information is a necessary and lacking key element for model development regardless of the form [algebraic (e.g., Speziale, 1999), one-equation (e.g., Johnson *et al.* (1994) or differential (e.g., Morrison, 1992)].

## **1.3 Research Objectives**

The purpose of this one-year project was to bridge the gap between an earlier AFOSR Grant (F49620-98-1-0038) and a follow-on AFOSR Grant (F49620-02-1-0365). In the earlier grant, the PI performed a detailed investigation of the effects of roughness ( $k^+ = 0-570$ , and  $M = 0.25, 0.67$  and  $2.8$ ) on flat-plates with low freestream turbulence ( $\sim 1\%$ ). The results of that study were disseminated to the Air Force through the final report, numerous



journal publications, contractor meetings and conference presentations; see Latin and Bowersox (1999, 2000, 2002), Fan and Bowersox (1999) and Pritchett and Bowersox (2001).

The principal focus of the follow-on project (F49620-02-1-0365) is improved understanding of the turbulent flow physics associated with surface roughness and freestream turbulence on the surface, mean and turbulent flow properties of non-equilibrium, strained (curvature driven), compressible, boundary layer flow with surface roughness and elevated freestream turbulence levels. An experimental and numerical research project was designed to provide (1) fundamental flow field understanding of non-equilibrium, strained, compressible, boundary layer flow with surface roughness and elevated freestream turbulence and (2) and pragmatic engineering information to the Air Force.

The objective of the interim grant (F49620-01-1-0115) was to continue progress in the rough-wall research area by designing, constructing and testing a series of Mach 3.0 favorable pressure gradient experimental test sections.

#### **1.4 Summary of Progress**

An initial 6-month delay was incurred due to an administrative problem at The University of Alabama. A 6-month extension was requested by the PI and granted by the AFOSR. The models were then designed and constructed (Chapter 4 describes the resulting models); however, this took approximately 10 months as compared to the anticipated 6 months. Hence, wind tunnel tests were not performed at The University of Alabama. However, the models transitioned to TAMU with the PI for completion of the

test matrix under a subcontract from The University of Alabama on the follow-on AFOSR project.

Because of the longer model manufacture time and to continue making progress towards the primary goal of the follow-on project, the PI initiated a numerical simulation effort originally planned for the follow-on research project. These numerical results will aid in the interpretation of the experimental data planned for the follow-on project.

### **1.5 Technology Transitions**

The technology transitions from this and the follow-on project are at two levels. First, the test matrix was defined based on practical Air Force requirements. Hence, the database itself is useful for model validation and practical engineering design. Second, fundamental information is planned with the goal of improved understanding of the flow physics, which will ultimately lead to improved prediction methods. As an example, the data generated in AFOSR Grant F49620-98-1-0038, as reported in Latin and Bowersox (2000) were used to validate numerical methods that are currently being used to design the hypersonic nozzle for the Air Force AEDC RDHWT/MARIAH II project.

## 2. Background Review

An abundance of research has been performed to quantify the effects of Mach number, roughness, freestream turbulence and wall curvature on turbulent boundary layers. However, studies of complex geometry flow that include measurements of second-order turbulence statistical moments are lacking; this finding is consistent with the recent article by Hefner (1999). However, a significant amount of relevant information concerning one or more of the parameters of interest is available, and is summarized below. The purpose of this section is to (1) present a representative sample of the database to identify prevalent findings and highlight results relevant to the present proposal and (2) outline the fundamental limitations for current prediction methods.

### 2.1 Smooth Flat Plate Turbulent Boundary Layers with Low Turbulence

Low-speed, smooth-wall, low freestream turbulence, zero-pressure-gradient boundary layer flow is understood to the point that flow fields are considered canonical and the semi-empirical correlations (law of the wall, defect law, and energy spectra scaling) and turbulent kinetic energy transport data are routinely used to validate turbulence modeling concepts. Numerous complete reviews of this subject are available [e.g., Schlichting (1979), Schetz (1993), White (1991), Sherman (1990) and Wilcox (1993)]. Repeating the discussion of incompressible, smooth, zero pressure boundary layer flow is not warranted. Compressible flows are not as understood. As first observed by Morkovin (1961), it appears that many of the differences in the turbulent statistical properties across supersonic and subsonic smooth plate boundary layers can be explained, or at least correlated, by the thermodynamic property variations across the layer. This observation, termed Morkovin's hypothesis, was based on flat plate data and the flat plate form of the kinetic energy

transport equations, and has provided the rationale for using incompressible turbulence models for flows up to Mach 5. Scaling for compressibility has been found to correlate the mean velocity with the low-speed database across smooth boundary layers [Van Driest (1951)]. More recently, detailed compilations and analyses of available high-speed turbulence smooth wall data [Fernholz *et al.* (1981), Smits *et al.* (1989), Spina *et al.* (1994), Dussuage *et al.* (1996) and Smits and Dussuage (1996)] have been performed. In summary, the studies indicated that the database was insufficient to confirm turbulent property scaling and the realm of applicability of Morkovin's hypothesis might be more restrictive than originally believed. In addition, supersonic flows often possess features that do not have incompressible counterparts; for example, shock-boundary layer interaction.

## 2.2 Rough Flat Plate Turbulent Boundary Layers with Low Turbulence

For low-speed rough-wall flows, the mean and turbulent flow properties are also well documented [Nikuradse (1933), Corrsin and Kistler (1955), Perry *et al.* (1969), Simpson (1973), Antonia and Wood (1975) and Schlichting (1979)], and the associated flow scaling has provided the foundation for turbulence models suitable for low-speed zero-pressure-gradient flow [Fan and Bowersox (1999) and Wilcox (1993)]. From the experimental descriptions, surface roughness has been shown to have a direct effect on the inner region of the law of the wall and is typically described by a single parameter; namely the roughness Reynolds number  $k^+$  ( $k^+ \equiv ku^*/\nu$ ). Three roughness regimes have been identified for low-speed flow [Aerodynamically smooth ( $k^+ < 4.5$ ), transitional ( $4.5 < k^+ < 60-70$ ) and fully rough ( $k^+ > 60-70$ )]. Nikuradse (1933) demonstrated that sand-grain generated roughness increased the velocity defect and skin friction and shifted the

logarithmic region of the law of the wall downward. However, the same defect law scaling was found to hold for rough and smooth walls. The amount of downward shift of the logarithmic region of the boundary layer was shown to be a function of  $k^+$ . Schlichting (1979) introduced the concept of equivalent sand-grain roughness  $k_s^+$  to correlate any surface roughness to the equivalent Nikuradse sand-grain roughness for comparison. The equivalent sand-grain roughness does not include roughness geometry or spacing. Thus, investigations of the influence of the roughness geometry have been performed [Perry *et al.* (1969), Simpson (1973), Antonia and Wood (1975)]. However, a satisfactory general treatment has not been presented.

The basic trend in the turbulence results of Corrsin and Kistler (1955) for a fully rough flow was that the axial turbulence intensity levels increased by about 30-40% and the Reynolds shear stresses increased by nearly a factor of 2. These data lead to obvious statement that roughness significantly alters the production and dissipation of turbulence. Grass (1971) concluded that a different dominant mode of near wall instability "might prevail" for rough walls. The laser Doppler velocimetry data of George and Simpson (2000) confirmed the defect law scaling and the shift in the logarithmic region of the boundary layer, and provided quantification of the bursting process.

Goddard (1959) and Berg (1979) found that for Mach numbers in the range of 0.7 - 6.0, the shift in the law of the wall velocity profile followed the same law as the incompressible case when the Van Driest  $II^{13}$  compressibility transformation was used. Latin and Bowersox (1999) also noted that when the roughness elements were observed to protrude into the supersonic portion of the boundary layer, the corresponding shock and expansion waves distorted the boundary edge. Liepmann and Goddard (1957) conjectured that for

fully rough flow, the wall shear force is primarily the result of the drag on the roughness elements. Based on this argument, they showed that the ratio of compressible to incompressible skin friction is equal to the wall-to-freestream density ratio. The force balance data of Goddard (1959) confirmed the Liepmann and Goddard skin friction correlation over a Mach number range of 0.7-4.54.

Latin and Bowersox (2000, 2002), Latin and Bowersox (1999), Fan and Bowersox (1999) and Pritchett and Bowersox (2001) extended the above database to include detailed turbulence information over a range of Mach numbers ( $M = 0.2 - 2.8$ ). A subset of important results that directly support the need for the present research is given here. Focusing only on the supersonic condition, the roughness elements were observed to protrude into the supersonic portion of the boundary layer, and the corresponding shock and expansion waves distorted the boundary edge and interacted with the boundary layer turbulence. The trends in the mean flow, observed for incompressible rough wall flow, were found to hold for the present study when Van Driest II scaling was used. In general, the rough wall kinematic statistical turbulent flow properties measured with the laser Doppler velocimetry system, collapsed on to a single curve when scaled with outer flow variables. The only exception was the 2-D plate, and it was expected that the turbulence production mechanisms associated with the d-type cavity were significantly different than for the remaining plates, which all had 3-D roughness patterns. Roughness was found to extend the region of inner scaling applicability for the kinematic properties further out into the boundary layer. The turbulent flow statistical properties with the explicit thermodynamic dependence did not collapse when scaled by local mean quantities, and increased almost linearly with  $k_s^+$ . The transverse-velocity-density correlation increased

rapidly with roughness height. It was shown that the influence of smaller roughness elements increased the skin frictional losses more than the boundary layer turbulence levels. However, as the roughness height was increased, the turbulence production relative to the frictional losses increased. The equivalent sand-grain roughness was found to be an effective parameter to characterize the overall effects of roughness on the turbulent flow properties. The machined 2-D and 3-D plate results were in reasonable agreement with the sand-grain trends, however significant variances (up to 25%) were observed and related back to roughness topology. Hence, it was concluded that the roughness topology was an important factor in the turbulence production. Three algebraic rough-wall turbulence models (van Driest, Kragstad and Cebeci-Chang) were tested. In summary, all three models produced mean, integral and turbulence results that agreed well with the experimental data.

### **2.3 Effect of Pressure Gradient/Wall Curvature on Smooth-Wall Boundary Layers**

Low-speed boundary layers with pressure gradients have also been the subjects of numerous investigations; e.g., reviews are presented in [Bradshaw (1973), Sherman (1990), White (1991) and Schetz (1993)]. In summary, the inner region boundary layer scaling (i.e., law of the wall) has been shown to hold in the presence favorable and adverse pressure gradients. The logarithmic region termination height has been shown to depend on the strength of the pressure gradient; for favorable pressure gradients, the height increases and for adverse pressure gradients it decreases. Near separation, the inner scaling breaks down. The outer region of the boundary layer is very sensitive to pressure gradient, and in general the defect law does not hold. However, Clauser (1956) defined a pressure gradient strength parameter ( $\beta$ ) as the product of the axial pressure gradient

( $dp/dx$ ) and the ratio of the boundary layer displacement thickness ( $\delta^*$ ) and wall shear stress ( $\tau_{wall}$ ) [i.e.,  $\beta = -(\delta^*/\tau_{wall})(dp/dx)$ ], and when  $\beta$  is constant, the boundary layers are in equilibrium; i.e., the defect scaling laws hold and the corresponding profiles are independent of axial location). Coles (1956) used this idea to generalize the law of the wake for equilibrium pressure gradient flows. For very strong adverse pressure gradients, the velocity profile is such that maximum shear stress moves away from the wall, and usual defect law scaling breaks down. Perry and Schofield (1969) introduced a new outer scaling law for strong adverse equilibrium and quasi-equilibrium (flows where the pressure gradients are mild enough that  $\beta$  depends only on local flow conditions) flows. Power law axial velocity distributions produce equilibrium (or quasi-equilibrium flows).

For laminar flow, concave surfaces can produce Görtler vortices [White (1991)]. Stable Görtler vortices have been documented as difficult to produce in fully turbulent flow with elevated freestream turbulence [Kestoras and Simon (1995)], and Smits and Dussauge (1996) describe a criterion to avoid the formation of Görtler vortices for low freestream turbulence levels.

As observed for diffusers and nozzles [Patel (1996)] favorable pressure gradients without wall curvature (i.e., accelerating flows) reduce turbulence levels; the opposite is true for adverse pressure gradients. Concave and convex curvature, with and without [Thomann (1968)] an associate pressure gradient, have been shown to have de-stabilizing and stabilizing effects, respectively, on the turbulent flow properties of across low-speed boundary layers [Bradshaw (1969, 1973)]. For convex curvature, the turbulence levels, turbulent shear stresses and wall friction all decrease relative to canonical flat surface values; the opposite is observed for concave curvature. These trends are explained by



simple angular momentum arguments. The angular momentum terms in the Navier-Stokes equations for planar flow over curved surfaces are on the order of the ratio of the boundary layer thickness and radius of curvature of the wall turning; hence, the effects are first order. For laminar flow, the effects have been shown to be first order [Patel (1996)]. However for turbulent flows, the effects of wall curvature are significantly larger (approximately a factor of 10) than expected, where heuristic empirical corrections are required to account for this effect in predictions [Bradshaw (1969, 1974)]. The effects of wall curvature are most pronounced in the outer region of the boundary layer, where for strong wall curvatures (e.g., ratio of the boundary thickness and wall radius of curvature of order 0.1), negative Reynolds shear stresses have been observed [Shivaprasad and Ramaprian (1978)]. Kim and Simon (1988) report that the turbulent heat flux was affected by curvature more than the turbulent shear stress.

Many of the observed differences between distorted supersonic and subsonic boundary layers can be explained in terms of the fluid property changes across the boundary layer [Spina *et al.* (1994), Smith and Smits (1994) and Bradshaw (1974)]. However, supersonic flows possess phenomena that do not have incompressible counterparts. For example, wave (expansion or compression) boundary layer interactions, where the longitudinal pressure gradients can lead to compression or dilatation, which in turn affect the velocity, pressure and density fluctuations, are not present in subsonic flow.

When a streamwise favorable pressure gradient is imposed on a supersonic boundary layer, the flow is distorted by both the effects of pressure gradient and by bulk dilatation. The ratio of the extra strain rates to the primary  $\partial u / \partial y$  velocity gradient, called the distortion parameter, has been used as a convenient means to classify a pressure gradient

[Bradshaw (1973)]. A distortion is generally considered mild if  $d_{max} \approx 0.01$  and strong for  $d_{max} \approx 0.1$  [Spina *et al.* (1994)]. If the distortion is applied for a time that is comparable to an eddy lifetime, then the impulse parameter (I), the time-integrated strain rate, may be a better choice [Smith and Smits (1994)]. For an impulsive perturbation resulting from a region of bulk compression,  $I_p = \ln(p_2/p_1)/\gamma$  [Smith and Smits (1994) and Hayakawa *et al.* (1984)]. For an impulse as a result of curvature,  $I_\phi = \Delta\phi$  [Smits *et al.* (1979)]. Even though the interactions between the strain rates are most likely nonlinear, the linear addition of the perturbation strengths is usually accepted for crude comparisons among different flows. Luker *et al.* (1998) present a generalization of the pressure gradient strength definition

Collectively, the available turbulence data [Donovan (1993), Smith and Smits (1991), Jarayam *et al.* (1987), Dussauge and Gaviglio (1987) and Thomann (1968)] indicate that the axial turbulence intensities decrease by 70-90% for  $I_p$  and  $I_\phi$  values  $\in (-0.4, -1.0)$  and  $(-0.1, -0.3)$ , respectively. Because of the reduction in the fluctuating properties, as well as reductions in the skin friction and heat transfer, favorable pressure gradients are often characterized as having a stabilizing effect. Relaminarization of part of the boundary layer is believed possible if the pressure gradient is strong enough [Spina *et al.* (1994) and Jarayam *et al.* (1987)]. Smith and Smits (1991) and Dussauge and Gaviglio (1987) estimated, using a rapid distortion analysis, that the majority of the turbulence reduction was the result of mean bulk dilatation.

Arnette *et al.* (1996) showed that the overall magnitude of the kinematic Reynolds shear stress was dramatically decreased across the entire boundary layer for 7.0 and 14.0 deg. centered and gradual expansions. They further defined an "apparent reverse

transition,” where the normal energy transfer from the mean flow had been reversed, to describe a sign changing of the Reynolds shear stress. Although the Arnette *et al.* study provided detailed turbulence information throughout the expansion, the axial spacing was not refined enough to resolve the stream wise strain rates.

Luker *et al.* (2000), Bowersox *et al.* (2000), Luker *et al.* (1998), and Bowersox and Buter (1996) performed detailed investigations of the influence of the wall curvature driven pressure gradients on the turbulent flow field including the turbulent shear stress transport. A subset of important results to support the need for the present research is listed here. Focusing only on the favorable pressure gradient flow, the turbulence data indicated that the present favorable pressure gradient had the expected stabilizing effect on the turbulent quantities. The magnitude of the Reynolds shear stress was also reduced by the favorable pressure gradient; in the near-wall region it was approximately 25% of the zero pressure gradient value, and in the outer region ( $y/\delta > 0.5$ ), the kinematic Reynolds shear stresses *were negative and the principle strain rates were positive*. The three-dimensional strain rate measurements and the associated extra production indicated that the overall turbulence production was also negative in the outer half of the favorable pressure gradient boundary layer. In addition, the use of a body-intrinsic coordinate system contributed to the reduced shear stress levels. Also, the present data collectively indicated that the favorable pressure gradient was disintegrating the large-scale eddies into smaller ones. This redistribution of energy increased the amount of turbulent energy available for dissipation by the flow, which in turn had the observed stabilizing effect on the boundary layer. Numerical simulations using two-equation turbulence modeling demonstrated that the eddy viscosity approach was inadequate for these very mild pressure gradient flows.

a 20% increase in freestream turbulence intensity. The degree to which the turbulent boundary layers are affected by freestream turbulence also depends on the structure of the freestream turbulence; specifically, the turbulent length scales [Bradshaw and Simonich (1978)]. The logarithmic regions of the boundary layer velocity and thermal profiles have been shown to be unaffected by freestream turbulence level and length scales [Blair (1983), Hancock and Bradshaw (1983), and Moss and Oldfield (1992)]. However, velocity and temperature profiles measured by Young *et al.* (1992) deviated from the low freestream turbulence cases when the freestream turbulence was generated with a blown grid; furthermore, the differences depended on the orientation of the blowing. Hancock and Bradshaw (1989) showed that the near wall dissipation length scale was unaffected by freestream turbulence, and hence the near wall production-dissipation balance held with elevated freestream turbulence levels.

The combined affect of nonzero pressure gradient and freestream turbulence has also received attention, albeit relatively little compared to zero-pressure-gradient flows. For example, Gostelow *et al.* (1994) present a detailed examination of the effects of freestream turbulence and adverse pressure gradient on boundary layer transition, where the onset and length of transition depended strongly on both the pressure gradient and freestream turbulence. For turbulent boundary layers Evans (1985) and Hoffmann and Mohammadi (1991) demonstrated that the Coles (1956) velocity profile wake function for adverse pressures is valid when a correction is applied for elevated freestream turbulence. In addition, Hoffmann and Mohammadi (1991) also correlated the skin friction by applying a freestream turbulence intensity parameter.

## 2.5 Limitations of Current Prediction Methods

The infeasibility of Direct Numerical Simulation (DNS) of practical high Reynolds number turbulent flow has been the subject of much discussion and research [e.g., see Salas *et al.* (1999) and Wilcox (2000)]. Hence, engineers and scientists must rely on approximate averaged forms of the governing Navier-Stokes equations. For Large-Eddy Simulation (LES) methods, a temporal filter is applied, the large-scale structures are simulated, and the influences of the small-scale structure are modeled. For the Reynolds or Favre averaged Navier-Stokes (RANS) approach [Wilcox (2000)], all of the turbulent temporal content is modeled. Due to the non-linearity of the Navier-Stokes equations, both filtering and averaging introduces additional second-order correlation unknowns into the problem. Modeling these additional unknowns has proven to be a major challenge and a limiting factor in the accuracy of high-Reynolds number numerical simulations.

By simulating the large-scale structures, large-eddy simulation techniques have the potential to bypass many of the challenges associated with the Reynolds averaged approach by minimizing a large portion of the models' influence on the accuracy of the numerical prediction. However, the influence of the subgrid model has proven to be very important [Bradshaw (1999)] especially for wall bounded flow, where near the wall, the solutions must approach DNS to minimize the effect of the subgrid model. Also, as computational power increases [Doligalski (1999)], most of the resources will be directed at multidisciplinary design of high-Reynolds number flow problems, as apposed to detailed large-eddy simulations. Hence, the Reynolds averaged approach will be prevalent for at least 20 years [Pope (1999)].

Specific to this project, numerous turbulence models for use in the Reynolds or Favre averaged form of the Navier-Stokes equations, with varying degrees of success [Johnson *et*

*al.* (1994) and Salas *et al.* (1999)], have been tried or formulated for flow over curved surfaces. From the numerous studies (note, a detailed data review was omitted because of the proposal page limitation) and survey articles it is clear that algebraic and two-equation eddy-viscosity models are not appropriate for nonequilibrium flow [e.g., Kassinos and Reynolds (1999)]. Nonlinear eddy-viscosity models can be calibrated to produce improved results, however the mathematical mechanisms for the improvement are different than the actual flow physics [Apsley *et al.* (1997) as discussed in Bradshaw (1999)], and hence, the models “may fail spectacularly.” It is well accepted that the second-order transport formulations are more realistic representations of the flow physics than any of the eddy-viscosity type formulations. However, as indicated by Bradshaw (1999): “Even stress-transport models often give poor predictions of complex flows - notoriously, the effects of streamline curvature are not naturally reproduced, and empirical fixes for this have not been very reliable.” The difficulty lies in the lack of understanding and modeling ability for many of the terms in the transport equations (e.g., dissipation, diffusion, pressure-strain redistribution, etc...), and this lack of understanding can be traced back to an inadequate database upon which the flow physics can be gleaned. The following quote from Hefner (1999) provides clear assessment of the current state of turbulence modeling and the available database:

"Much of the turbulence modeling research has focused on modeling the effect of turbulence on mean flows rather than modeling the turbulence physics; therefore, much of the turbulence modeling effort has focused on tweaking or adding constants and terms in the models to predict the available experimental data, which

too often is mean flow data and not turbulence data. Although much has been said over the years regarding the need for definitive turbulence modeling experiments, there remains a paucity of high quality dynamic turbulence data useful for modeling and validation for flows about complex geometries."

diffusion formulation, and turbulent diffusion, modeled with an isotropic version of Launder *et al.* (1975). Lastly, the dissipation was modeled following Hanjalic and Launder (1976) and Sarkar *et al.* (1989). The model formulation, along with near wall corrections, is given in Morrison (1992). Wilcox (2000) also summarizes the formulations for two additional turbulent transport models, where the principle differences are associated with the pressure-strain-rate tensor formulation.

An in-house code (CFVPNS), written by Dr. Bowersox is being used to assess an array of algebraic roughness models (described in Chapter 4). The cell-centered, finite volume parabolized Navier-Stokes CFD code, which utilizes generalized curvilinear coordinates, Roe's scheme and a 4-stage Runge-Kutta time integration, is briefly described in Bowersox (1996). The industry code GASP (Aerosoft, Inc.) is also currently being used to assess the rough-wall  $k-\omega$  model described in Wilcox (2002).



## 4. Results

The work during this one-year effort focused on the design and construction of the supersonic favorable pressure gradient wind tunnel models and preliminary numerical simulations. This section describes the results from these two efforts.

### 4.1 Wind Tunnel Models

Interactions between the PI and Dr. Beutner (the AFOSR program manager) led to an extended roughness topology test matrix, where the originally proposed roughness topologies consisting of square pillar elements was increased to include axial grooves, lateral grooves and diamond shaped pillars. Thus, the test matrix increased from four wind tunnel models [two flat and two convex plates (smooth and rough with square pillars) to ten models [five flat and five convex plates (smooth, square pillars, axial grooves, lateral grooves and diamond pillars)]. The models were designed and constructed, however slow manufacture time resulted in about a 10 month design and construct cycle. Hence, testing was not accomplished at The University of Alabama. The PI accepted a position at Texas A&M University, and a joint UA-TAMU follow-on project has been awarded. The experimental portion of the project will now take place at TAMU, and the numerical work will continue at the UA under the direction of Dr. M. Sharif. Hence, the wind tunnel models transitioned to TAMU to complete the follow-on project. A description of the models is given below.

Shown in Fig. 1 is a schematic of the experimental test-section designed and constructed for this project (favorable-pressure-gradient wall shown). The wind tunnel facilities are described in Chapter 3. The test locations are to be located downstream of a fully characterized, equilibrium, zero-pressure-gradient turbulent boundary layer. An

angled upper surface was designed to adjust the pressure gradient strength so that the incoming boundary layer has a negligible pressure gradient over the length of the test section leading to the curved wall region. A zero-pressure-gradient model will be tested to provide a canonical baseline.

The models were constructed from Plexiglas to minimize laser reflections for the PIV measurements. Photographs for all of the roughness topologies are shown in Fig. 2 (convex wall shown). The grooves were machined to a depth of 0.79 mm (1/32") with a 0.79 mm (1/32") radius ball end mill; the uncertainty in the roughness height (based on milling machine specifications) is 0.025 mm (0.001"). Shown in Fig. 3 is a sketch of the groove pattern (depth and shape), which was used for all of the models. The diamond pattern was machined such that the diamond half-angle is 20°, the minor axis dimension at the top of the roughness element is 3.175 mm (1/8"), and the minor axis is normal to the flow direction. The dimensions of the square roughness elements at the top are 3.175 mm x 3.175 mm (1/8" x 1/8"). The lateral groove elements are 3.175 mm (1/8") wide at the top of the element, and the span the tunnel width. The longitudinal elements are similar to the lateral, however they span the length of the model in the flow direction.

The favorable pressure gradient wall geometry is shown schematically (to scale) in Fig. 4. Table 3 lists the coordinates used in the computer controlled milling of the models. For numerical simulations, the wall geometry (Table 3) was fit by the following curve:

$$y = \begin{cases} 0, & 0 \leq x \leq 26 \\ -1.004 \times 10^{-4} \cdot x^5 + 2.174 \times 10^{-3} \cdot x^4 - 1.325 \times 10^{-2} \cdot x^3 \\ \quad + 8.997 \times 10^{-3} \cdot x^2 - 1.918 \times 10^{-2} \cdot x & 26 < x < 38 \end{cases}$$

where the units are in inches,  $R^2 = 0.9999$  and the maximum error is  $5 \times 10^{-3}$  inches.

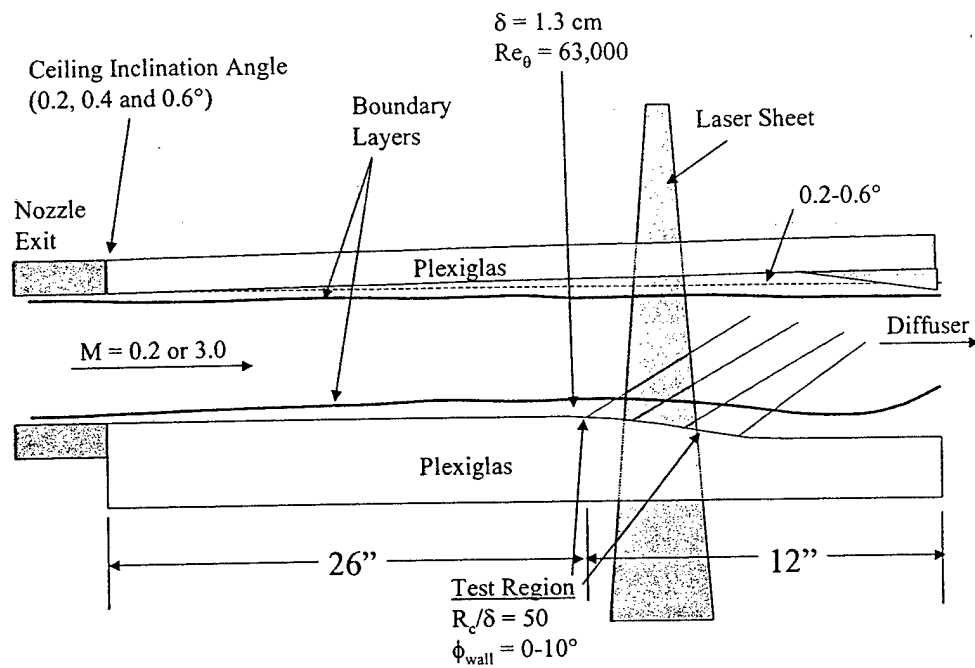
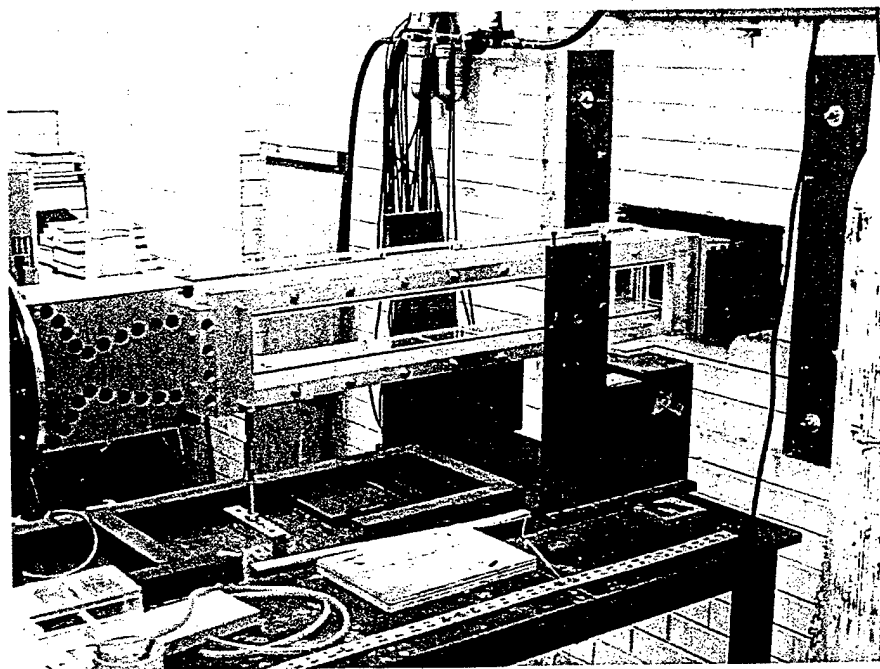
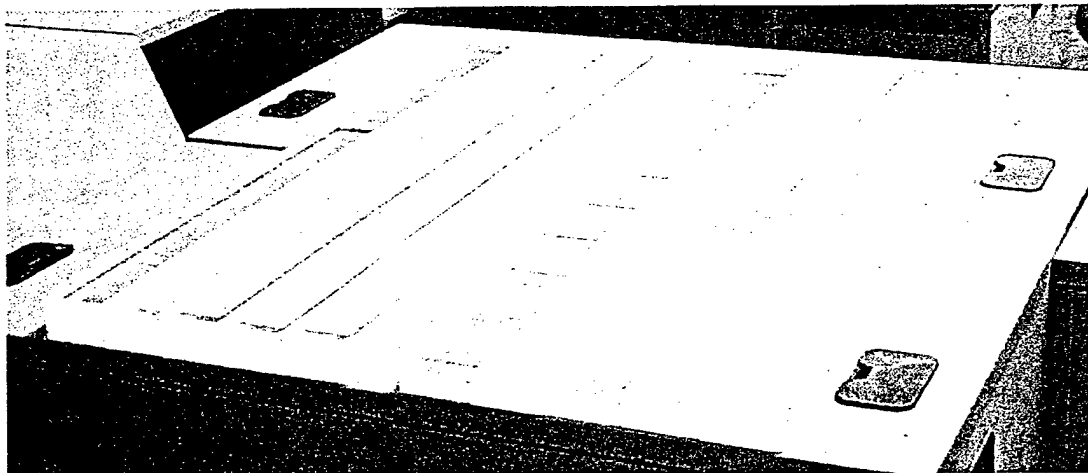


Figure 1 Flow Field Schematic



(2a) Test Section



(2b) Zero and FPG Models



Smooth Diamond Square Lateral Longitudinal

(2c) Roughness Patterns (flow direction from top to bottom)

Figure 2 Photographs of the Test Section and Surface Roughness Topologies

*(The pattern in the smooth plate is that of the table on which the plate was resting.)*

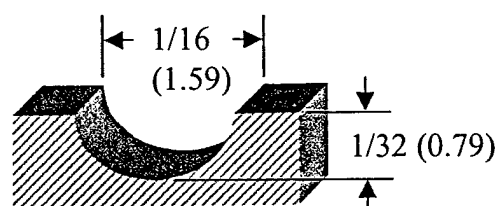


Figure 3 Semi-circular groove pattern for all of the roughness elements [in, (mm)]

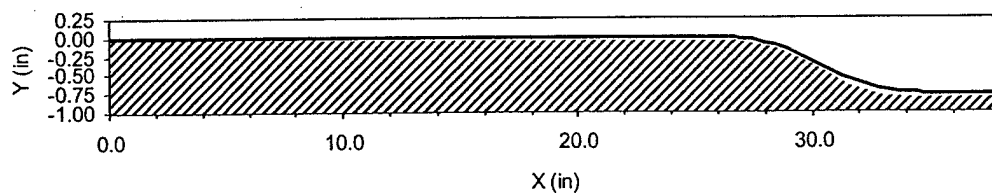


Figure 4 Favorable Pressure Wall Geometry

**Table 2 Favorable Pressure Gradient Wall Coordinates**

<b>X (inch)</b>	<b>Y (inch)</b>
1.13687E-13	0.00000E+00
1.29977E+01	0.00000E+00
2.59953E+01	0.00000E+00
2.60000E+01	0.00000E+00
2.64847E+01	-4.74364E-03
2.69691E+01	-1.88819E-02
2.74532E+01	-4.24094E-02
2.79368E+01	-7.53173E-02
2.84196E+01	-1.17593E-01
2.89015E+01	-1.69221E-01
2.93824E+01	-2.30182E-01
2.98619E+01	-3.00453E-01
3.03400E+01	-3.80007E-01
3.08181E+01	-4.59557E-01
3.12976E+01	-5.29824E-01
3.17784E+01	-5.90782E-01
3.22603E+01	-6.42408E-01
3.27431E+01	-6.84682E-01
3.32267E+01	-7.17589E-01
3.37108E+01	-7.41116E-01
3.41952E+01	-7.55255E-01
3.46798E+01	-7.60000E-01
3.46798E+01	-7.60000E-01
3.51541E+01	-7.60000E-01
3.56285E+01	-7.60000E-01
3.61028E+01	-7.60000E-01
3.65771E+01	-7.60000E-01
3.70514E+01	-7.60000E-01
3.75257E+01	-7.60000E-01
3.80000E+01	-7.60000E-01

## 4.2 Numerical Results

Van Driest proposed a vortex generation idea to account for roughness where, when a state of complete roughness is reached, the viscous effect of the wall is eliminated. From a mathematical view, he presented his formula by adding a vortex generation term. The vortex generation term grows with size of roughness in the form of  $\exp(-R^+y^+/A^+k^+)$  such that when  $y^+ = k^+ = 60$ . Thus, the van Driest model is given by

$$l_m = ky \left[ 1 - \exp(-y^+ / 26) + \exp(-y^+ R^+ / 26k^+) \right]$$

where  $R^+ = 60$ .

Kragstad presented a modified damping function similar to that of Van Driest, where in the damping function the term  $(R^+ / k^+)$  was taken to 3/2 power, and  $R^+ = 70$ . For higher values of  $k^+$ , a square root term was added to increase the mixing. Thus, the Kragstad formula for the mixing length is

$$l_m = 0.085\delta \tanh\left(\frac{\kappa y}{0.085\delta}\right) \{ 1 - \exp(-y / A^+) + \exp[-y^+ / A^+ (R^+ / k^+)^{3/2}] \} \sqrt{1 + \exp(-R^+ / k^+)}$$

The model used by Cebeci-Chang is somewhat different than the two described above, where a displacement  $\Delta y$  related to the averaged roughness height is defined, and the velocity profile is obtained by a shift of the smooth wall profile. To generate the analogous smooth plate profile, the reference plane was shifted in the opposite direction to main flow. Based on the law of wall and the mixing length formulation, a displacement formula relative to roughness was obtained. Thus, the mixing length was modified by a displacement to account for the roughness effect as follows

$$l_m^+ = \kappa (y^+ + \Delta y^+) \{ 1 - \exp[-(y + \Delta y)^+ / A^+] \}$$

$$\Delta y^+ = 0.9 [\sqrt{k_S^+} - k_S^+ \exp(-k_S^+ / 6)]$$

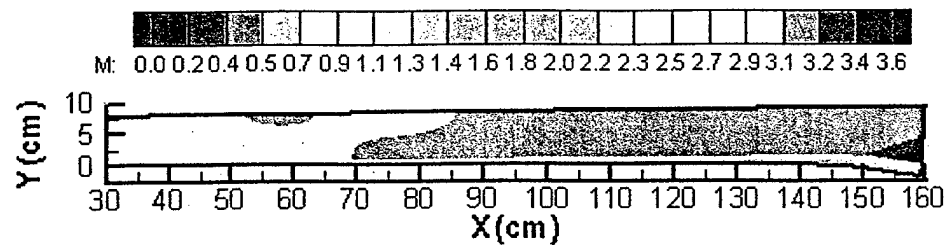
$$4.535 < k_S^+ < 2000.$$

To date the van Driest model has been incorporated into CFVPNS, along with the compressible forms of the Prandtl and Clauser models described in Cebeci-Smith (1974).

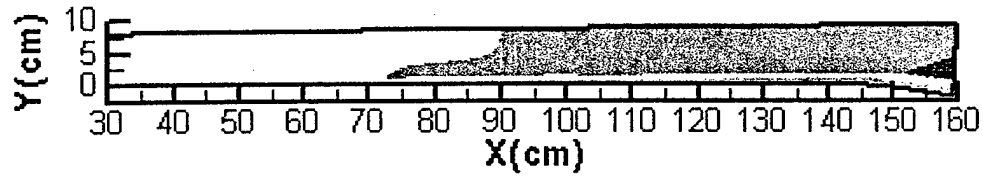
Shown in Figs. 5a and b are the Mach number contours for the entire test section (smooth and rough) with a 0.6-degree divergence on the upper wall. For the rough wall calculation, the equivalent roughness height was fixed at 0.79 mm, and the predicted equivalent sand grain roughness ( $k_s^+$ ) was nominally 400 throughout the expansion region. The predicted freestream Mach number increased by 3.0-4.0% along the test section for both of these cases. However, only the lower wall viscous effects were included, and the divergence was designed to compensate for boundary layer growth on all four walls. Thus, the slight increase was expected.

The turbulence shear stress predictions using Prandtl's mixing length model, with and without the Van Driest roughness correction are given in Figs. 6a and b. The smooth plate results show the expected reduction in shear stress through the expansion region. Higher shear stress levels (20%) and a thicker boundary layer (15%) were predicted.

Given in Fig. 7 are the predicted law-of-the-wall plots using the  $k-\omega$  turbulence model. The current formulation requires  $k_s^+$  as an input. Hence, the code was run for a range of values expected in the present experiments (0, 100 and 500 shown here). The expected velocity shift is observed.

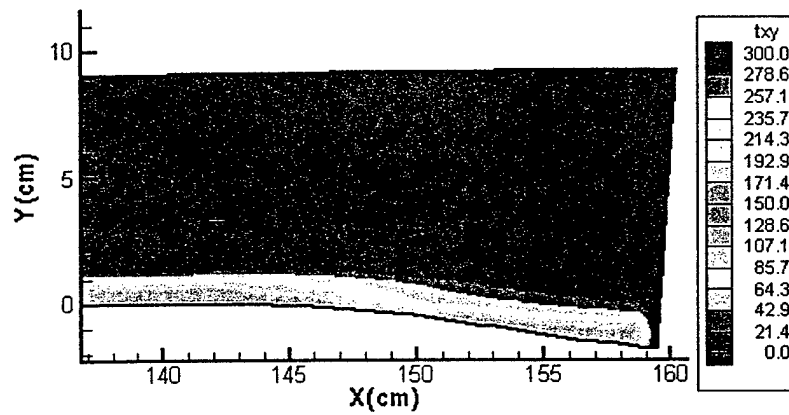


(5a) Smooth

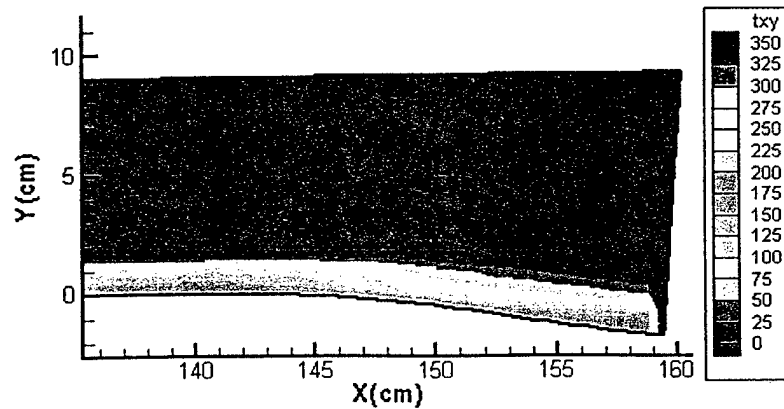


(5b) Rough ( $k = 0.79$  mm)

Figure 5 Mach Distributions within the FPG Test Sections



(6a) Smooth



(6b) Rough ( $k = 0.79$  mm)

Figure 6 Shear Stress Distributions (Algebraic Models)



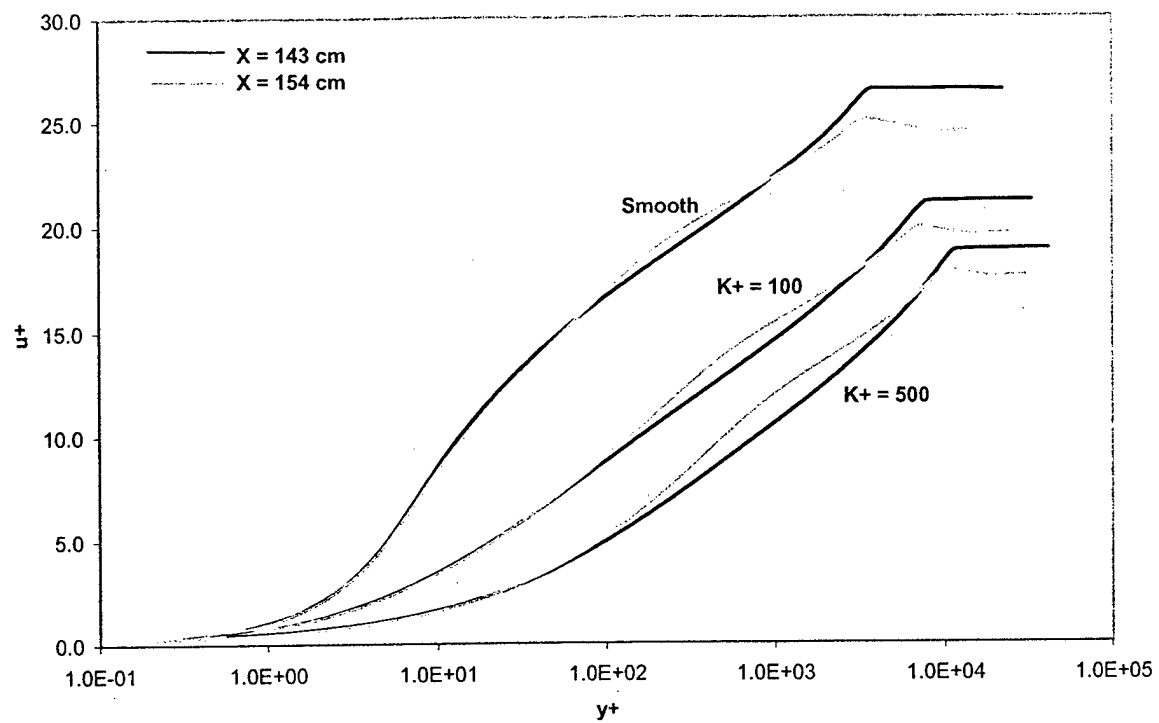


Figure 7 Law-of-the-Wall Results,  $k-\omega$  model without compressibility scaling)

## 5. Bibliography

- Apsley, D., Chen, W.-L., Leschziner, M. and Lien, F.-S., "Non-Linear Eddy-Viscosity Modelling of Separated Flows," *J. Hydraulic Res.*, Vol. 35, 1997, p. 723.
- Arnette, S. A., Samimy, M. and Elliott, G. S., "The effects of Expansion Regions on the Turbulence Structure of Compressible Boundary Layers," AIAA Paper 96-0656, Jan. 1996.
- Air Force, *New World Vistas, Aircraft and Propulsion Technologies*, 1995.
- Air Force Office of Scientific Research, *Research Interests Of The Air Force Office Of Scientific Research And Broad Agency Announcement 2000-1*, AFOSR 64-1, Department Of The Air Force, Air Force Office of Scientific Research (AFRL), 801 North Randolph Street, Room 732, Arlington VA 22203-1977, June 1999.
- Bowersox, R., and Buter, T., "Mass-Weighted Turbulence Measurements in a Mach 2.9 Boundary Layer with Mild Adverse and Favorable Pressure Gradient," *AIAA Journal*, Vol. 34, No. 12, 1996, pp. 2470-2483.
- Bowersox, R., Wier, R., Glawe, D., and Gogineni, S., "Measurements of Turbulent Flow Structure in Supersonic Curved Wall Boundary Layers," *Journal of Propulsion and Power*, Vol. 16, No. 1, 2000, pp. 153-154.
- Bradshaw, P., "The Best Turbulence Model for Engineers," *Modeling Complex Flows*, Ed. by Salas, D., Hefner, J. and Sakell, L., ICASE/LaRC, Kluwer Academic Publishers, Boston, 1999.
- Cebeci, Tuncer and Smith, A. M. O. *Analysis of Turbulent Boundary Layers*. Applied Mathematics and Mechanics, Academic Press, 1974.
- Chenault, L., Beran, P., and Bowersox, R., "Second-Order Reynolds Stress Turbulence Modeling of Three-Dimensional Oblique Supersonic Injection," *AIAA Journal*, Vol. 37, No. 10, 1999, pp. 1257-1269.
- Doligalski, T., "Army Turbulence Modeling Needs," *Modeling Complex Flows*, Ed. by Salas, D., Hefner, J. and Sakell, L., ICASE/LaRC, Kluwer Academic Publishers, Boston, 1999.
- Durst, F., Melling, A., and Whitelaw, J., *Principles and Practice of Laser-Doppler Anemometry*, Academic Press, New York, 1981.
- Fan, H. and Bowersox, "Numerical Analysis of High-Speed Flow over Rough Surfaces," AIAA-99-2381, 35<sup>th</sup> AIAA/ASME/SAE/ASEE Joint Propulsion Conference, Los Angeles CA, June 1999.
- Hanjalic, K and Launder, B., "Contribution Towards a Reynolds-Stress Closure for Low-Reynolds-Number Turbulence," *Journal of Fluid Mech.*, Vol 74, pt. 4, 1976, pp. 593-610.
- Hazelton, D., Bowersox, R., Nuemann, D., and Hayes, J., "Skin Friction Measurements in a Mach 6 Inlet Test," AIAA-97-2884, 33rd AIAA/ASME/SAE/ASEE Joint Propulsion Conference, Seattle WA, July 6-9, 1997.
- Hefner, J., "Current and Future Needs in Turbulence Modeling," *Modeling Complex Flows*, Ed. by Salas, D., Hefner, J. and Sakell, L., ICASE/LaRC, Kluwer Academic Publishers, Boston, 1999.
- Hinze, O., *Turbulence*, McGraw-Hill, New York, 1975.

- Johnson, D., Mentor, F., and Rumsey, C., "The Status of Turbulence Modeling for External Aerodynamics," AIAA 94-2226, June 1994.
- Kassinis, S., and Reynolds, W., "Developments in Structure-based Turbulence Modeling," *Modeling Complex Flows*, Ed. by Salas, D., Hefner, J. and Sakell, L., ICASE/LaRC, Kluwer Academic Publishers, Boston, 1999.
- Lakshminarayana, B., *Fluid Dynamics and Heat Transfer of Turbomachinery*, John Wiley & Sons, New York, 1996.
- Turner, A. and Tarada, F. and Bayley, F., *Effects of Surface Roughness on Heat transfer to Gas Turbine Blades*, AGARD CP 390, 1985.
- Latin, R. and Bowersox, R., "Temporal Turbulent Flow Structure for Supersonic Rough-Wall Boundary Layers," *AIAA Journal*, Vol. 40, No. 5, 2002, pp. 832-841.
- Latin, R. and Bowersox, R., "Flow Properties of a Supersonic Boundary Layer with Wall Roughness," *AIAA Journal*, Vol. 38, No. 10, 2000, pp. 1804-1821.
- Latin, R. and Bowersox, R., "Influence of Surface Roughness on Supersonic Boundary Layer Turbulent Flow Structure," Paper No. 99-7059, *14<sup>th</sup> International Symposium on Airbreathing Engines (XIV ISABE)*, Florence, Italy, Sept. 5-10, 1999a.
- Launder, B., Reece, G., and Rodi, W., "Progress in the Development of a Reynolds-Stress Turbulence Closure," *J. of Fluid Mech.*, Vol. 68, Pt. 3, 1975, pp. 537-566.
- Luker, J., Bowersox, R., Buter, T., "Influence of A Curvature Driven Favorable pressure gradient on a supersonic turbulent boundary layer," *AIAA Journal*, Vol. 38, No. 8, 2000, pp. 1351-1359.
- Luker, J., Hale, C., and Bowersox, R., "Experimental Characterization of the Turbulent Shear Stresses for Distorted Supersonic Boundary Layers," *Journal of Propulsion and Power*, Vol. 14, No. 1, 1998, pp. 110-118.
- Morrison, J., *A Compressible Navier Stokes Solver with Two-Equation and Reynolds Stress Turbulence Closure Models*, NASA CR 4440, 1992.
- Pope, S. "A Perspective on Turbulence Modeling," *Modeling Complex Flows*, Ed. by Salas, D., Hefner, J. and Sakell, L., ICASE/LaRC, Kluwer Academic Publishers, Boston, 1999.
- Pritchett, V. and Bowersox, R., "Flow Properties of Compressible and Incompressible Subsonic Turbulent Boundary Layers with Surface Roughness," *39<sup>th</sup> AIAA Aerospace Sciences Meeting*, Reno NV, Jan 2001.
- River, D., *Personal Communication*, 2000.
- Salas, M., Hefner, J. and Sakell, L., *Modeling Complex Turbulent Flows*, ICASE/LaRC Interdisciplinary Series in Science and Engineering, Kluwer Academic Publishers, 1999.
- Sarkar, S., Erlebacher, G., Hussaini, M. and Kreiss, H., "The Analyses and Modeling of Dilatational Terms in Compressible Turbulence," ICASE Report 89-79, Univ. Space Res. Assoc., Hampton, VA, 1989.
- Sherman, F., *Viscous Flow*, McGraw-Hill, New York, 1991.
- Simonich, J. and Bradshaw, P., "Effect of Freestream Turbulence on Heat Transfer Through a Turbulent Boundary Layer," *J. of Heat Trans.*, Vol. 100, pp. 671-676.
- Smits, A. and Dussauge, J-P., *Turbulent Shear Layers in Supersonic Flow*, American Institute of Physics, Woodbury New York, 1996.

- Smits, A. J., Spina, E. F., Alving, A. E., Smith, R. W., Fernando, E. M., and Donovan, J. F. "A Comparison of the Turbulence Structure of Subsonic and Supersonic Boundary Layers," *Physics of Fluids*, A Vol. 1 No. 11, 1989, pp. 1865-1875.
- Smits, A., Young, S., and Bradshaw, P., "The Effects of Short Regions of High Surface Curvature on Turbulent Boundary Layers," *Journal of Fluid Mechanics*, Vol. 94, Sept. 1979, pp. 209-242.
- Speziale, G., "Modeling Non-Equilibrium Turbulent Flows," *Modeling Complex Turbulent Flows*, Ed. Sales, Hefner and Sakell, Kluwer Academic Publishers, Boston, MA, 1999.
- Turner, A., Tarada, F. and Bayley, F., "Effects of Surface Roughness on Heat Transfer of Gas Turbine Engines," AGARD CP 390, 1990.
- Wilcox, D., *Turbulence Modeling for CFD*, 2<sup>nd</sup> Ed., DCW Industries, Inc., La Canada, California, 2000.
- Young, C., Han, J., Huang, Y. and River, R., "Influence of Jet-grid Turbulence on Flat Plate Boundary Layers Flow and Heat Transfer," *Journal of Heat Transfer*, Vol. 114, Feb, 1992, pp. 65-72.
- Zhang, H., So, R., Gatski, T., and Speziale, C., "A Near-Wall Second Order Closure Compressible Turbulent Flows," *Near Wall Turbulent Flows*, Ed. By So, Speziale and Launder, Elsevier, New York, 1993, pp. 209-218.